A&A 554, A72 (2013)
DOI: 10.1051/0004-6361/201220996

Astronomy & Astrophysics

Discovery of high and very high-energy emission from the BL Lacertae object SHBL J001355.9–185406

H.E.S.S. Collaboration, A. Abramowski[1], F. Acero[2], F. Aharonian[3,4,5], A. G. Akhperjanian[6,5], E. Angüner[7], G. Anton[8], S. Balenderan[9], A. Balzer[10,11], A. Barnacka[12], Y. Becherini[13,14,15], J. Becker Tjus[16], K. Bernlöhr[3,7], E. Birsin[7], E. Bissaldi[17], J. Biteau[15,⋆], C. Boisson[18], J. Bolmont[19], P. Bordas[20], J. Brucker[8], F. Brun[3], P. Brun[21], T. Bulik[22], S. Carrigan[3], S. Casanova[23,3], M. Cerruti[18,24], P. M. Chadwick[9], R. Chalme-Calvet[19], R. C. G. Chaves[21,3], A. Cheesebrough[9], M. Chrétien[19], S. Colafrancesco[25], G. Cologna[13], J. Conrad[26], C. Couturier[19], M. Dalton[27,28], M. K. Daniel[9], I. D. Davids[29], B. Degrange[15], C. Deil[3], P. deWilt[30], H. J. Dickinson[26], A. Djannati-Ataï[14], W. Domainko[3], L. O'C. Drury[4], G. Dubus[31], K. Dutson[32], J. Dyks[12], M. Dyrda[33], T. Edwards[3], K. Egberts[17], P. Eger[3], P. Espigat[14], C. Farnier[26], S. Fegan[15], F. Feinstein[2], M. V. Fernandes[1], D. Fernandez[2], A. Fiasson[34], G. Fontaine[15], A. Förster[3], M. Füßling[11], M. Gajdus[7], Y. A. Gallant[2], T. Garrigoux[19], H. Gast[3], B. Giebels[15], J. F. Glicenstein[21], D. Göring[8], M.-H. Grondin[3,13], M. Grudzińska[22], S. Häffner[8], J. D. Hague[3], J. Hahn[3], J. Harris[9], G. Heinzelmann[1], G. Henri[31], G. Hermann[3], O. Hervet[18], A. Hillert[3], J. A. Hinton[32], W. Hofmann[3], P. Hofverberg[3], M. Holler[11], D. Horns[1], A. Jacholkowska[19], C. Jahn[8], M. Jamrozy[35], M. Janiak[12], F. Jankowsky[13], I. Jung[8], M. A. Kastendieck[1], K. Katarzyński[36], U. Katz[8], S. Kaufmann[13], B. Khélifi[15], M. Kieffer[19], S. Klepser[10], D. Klochkov[20], W. Kluźniak[12], T. Kneiske[1], D. Kolitzus[17], Nu. Komin[34], K. Kosack[21], S. Krakau[16], F. Krayzel[34], P. P. Krüger[23,3], H. Laffon[27,15], G. Lamanna[34], J. Lefaucheur[14], M. Lemoine-Goumard[27], J.-P. Lenain[19], D. Lennarz[3], T. Lohse[7], A. Lopatin[8], C.-C. Lu[3], V. Marandon[3], A. Marcowith[2], G. Maurin[34], N. Maxted[30], M. Mayer[11], T. J. L. McComb[9], M. C. Medina[21], J. Méhault[27,28], U. Menzler[16], M. Meyer[1], R. Moderski[12], M. Mohamed[13], E. Moulin[21], T. Murach[7], C. L. Naumann[19], M. de Naurois[15], D. Nedbal[37], J. Niemiec[33], S. J. Nolan[9], L. Oakes[7], S. Ohm[32,38], E. de Oña Wilhelmi[3], B. Opitz[1], M. Ostrowski[35], I. Oya[7], M. Panter[3], R. D. Parsons[3], M. Paz Arribas[7], N. W. Pekeur[23], G. Pelletier[31], J. Perez[17], P.-O. Petrucci[31], B. Peyaud[21], S. Pita[14], H. Poon[3], G. Pühlhofer[20], M. Punch[14], A. Quirrenbach[13], S. Raab[8], M. Raue[1], A. Reimer[17], O. Reimer[17], M. Renaud[2], R. de los Reyes[3], F. Rieger[3], L. Rob[37], S. Rosier-Lees[34], G. Rowell[30], B. Rudak[12], C. B. Rulten[18], V. Sahakian[6,5], D. A. Sanchez[3,⋆], A. Santangelo[20], R. Schlickeiser[16], F. Schüssler[21], A. Schulz[10], U. Schwanke[7], S. Schwarzburg[20], S. Schwemmer[13], H. Sol[18], G. Spengler[7], F. Spieß[1], Ł. Stawarz[35], R. Steenkamp[29], C. Stegmann[11,10], F. Stinzing[8], K. Stycz[10], I. Sushch[7,23], A. Szostek[35], J.-P. Tavernet[19], R. Terrier[14], M. Tluczykont[1], C. Trichard[34], K. Valerius[8], C. van Eldik[8], G. Vasileiadis[2], C. Venter[23], A. Viana[3], P. Vincent[19], H. J. Völk[3], F. Volpe[3], M. Vorster[23], S. J. Wagner[13], P. Wagner[7], M. Ward[9], M. Weidinger[16], R. White[32], A. Wierzcholska[35], P. Willmann[8], A. Wörnlein[8], D. Wouters[21], M. Zacharias[16], A. Zajczyk[12,2], A. A. Zdziarski[12], A. Zech[18], and H.-S. Zechlin[1]

(Affiliations can be found after the references)

Received 23 December 2012 / Accepted 2 April 2013

ABSTRACT

The detection of the high-frequency peaked BL Lac object (HBL) SHBL J001355.9–185406 ($z = 0.095$) at high (HE; 100 MeV $< E <$ 300 GeV) and very high-energy (VHE; $E >$ 100 GeV) with the *Fermi* Large Area Telescope (LAT) and the High Energy Stereoscopic System (H.E.S.S.) is reported. Dedicated observations were performed with the H.E.S.S. telescopes, leading to a detection at the 5.5σ significance level. The measured flux above 310 GeV is $(8.3 \pm 1.7_{\rm stat} \pm 1.7_{\rm sys}) \times 10^{-13}$ photons cm^{-2} s^{-1} (about 0.6% of that of the Crab Nebula), and the power-law spectrum has a photon index of $\Gamma = 3.4 \pm 0.5_{\rm stat} \pm 0.2_{\rm sys}$. Using 3.5 years of publicly available *Fermi*-LAT data, a faint counterpart has been detected in the LAT data at the 5.5σ significance level, with an integrated flux above 300 MeV of $(9.3 \pm 3.4_{\rm stat} \pm 0.8_{\rm sys}) \times 10^{-10}$ photons cm^{-2} s^{-1} and a photon index of $\Gamma = 1.96 \pm 0.20_{\rm stat} \pm 0.08_{\rm sys}$. X-ray observations with *Swift*-XRT allow the synchrotron peak energy in νF_ν representation to be located at ∼1.0 keV. The broadband spectral energy distribution is modelled with a one-zone synchrotron self-Compton (SSC) model and the optical data by a black-body emission describing the thermal emission of the host galaxy. The derived parameters are typical of HBLs detected at VHE, with a particle-dominated jet.

Key words. BL Lacertae objects: individual: SHBL J001355.9-185406 – gamma rays: general

⋆ Corresponding authors: e-mail: david.sanchez@mpi-hd.mpg.de; biteau@in2p3.fr

1. Introduction

Observations of blazars in γ-rays offer the unique possibility to probe one of the most violent phenomena in the Universe. Blazars are active galactic nuclei (AGN) with their jets pointing towards the observer (Urry & Padovani 1995). Two classes have been distinguished (see e.g. Giommi et al. 2012; Ghisellini 2011): the flat spectrum radio quasars (FSRQ) are the most powerful blazars and their optical spectra exhibit absorption and emission lines, whereas the BL Lacertae (BL Lac) class is less luminous and presents weaker emission lines, with the equivalent widths of the strongest ones smaller than 5 Å (Stickel et al. 1991; Stocke et al. 1991).

Since the discovery of the first extragalactic source in the VHE domain (Mrk 421, Punch et al. 1992), the number of detected objects increased from a few in early 2000 up to 50 objects at the beginning of 2013 (see TeVCat[1] for an up-to-date overview.). The advent of the current generation of atmospheric Cherenkov telescopes (H.E.S.S., VERITAS, MAGIC) and the subsequent gain in sensitivity permit the detection of fainter and more distant sources. The efforts spent on understanding the properties of blazars and predicting VHE emission (Costamante & Ghisellini 2002; Massaro et al. 2008; Abdo et al. 2010a), together with measurements in the high-energy (HE; 100 MeV < E < 300 GeV) range, greatly contribute to the detection of new sources.

The spectral energy distribution (SED) of blazars is bimodal with one bump at low energy (from radio up to X-rays) and one at higher energy (from X-rays to TeV). BL Lac objects are further divided into two subclasses depending on the ratio between the X-ray and the radio fluxes (Padovani & Giommi 1995): the low-frequency peaked BL Lac objects with a peak below UV wavelengths and the high-frequency peaked BL Lac (HBL) objects for which the peak is in the UV or X-ray range. The latter subclass represents the bulk of the currently known extragalactic VHE γ-ray emitters detected by atmospheric Cherenkov telescopes (34 out of 50 early 2013), and almost 50% of the second *Fermi* catalogue of HE AGN (2LAC, Ackermann et al. 2011).

The low-energy bump of the SED is attributed to synchrotron emission of relativistic leptons (e^+e^- pairs) moving along the jet. The origin of the high-energy component is less definite. Leptonic models invoke inverse Compton (IC) scattering on either the synchrotron photons (synchrotron self-Compton, e.g. Band & Grindlay 1985) or an external photon field (external Compton, e.g. Dermer & Schlickeiser 1993). The γ-rays can also be produced by hadronic interactions, such as photoproduction of pions (e.g. Mannheim 1993) or synchrotron emission of protons (e.g. Aharonian 2000).

First detected in X-rays with ROSAT (1RXS J001356.6–185408, Voges et al. 1996), SHBL J001355.9–185406 was later identified as a BL Lac object by Schwope et al. (2000). With a radio flux of 29.6 mJy at 1.4 GHz (Condon et al. 1998) and an X-ray flux, between 0.1–2.4 keV, of 1.26×10^{-11} erg cm^{-2} s^{-1} (Voges et al. 1996), it fulfilled the selection criteria of the sedentary survey of extreme high-energy peaked BL Lacs (SHBL, Giommi et al. 2005), making this source a member of the HBL subclass.

Its relative proximity (z = 0.095, Jones et al. 2009) and its X-ray and radio fluxes are criteria that make SHBL J001355.9–185406 an interesting target for very high-energy (VHE, E > 100 GeV) observations (Costamante & Ghisellini 2002). Consequently, the source was observed with the High Energy Stereoscopic System (H.E.S.S.) and indeed reported as a TeV γ-ray emitter in November 2010 (Hofmann 2010).

The *Fermi* Large Area Telescope (LAT), launched on June 11, 2008, did not detect a high-energy (HE; 100 MeV < E < 300 GeV) counterpart after two years of operation (*Fermi* two-year catalogue, 2FGL, Nolan et al. 2012). However, the analysis of 3.5 years of data reported here reveals the presence of a faint source that is positionally coincident with SHBL J001355.9–185406.

The H.E.S.S. and *Fermi*-LAT data analyses and results are presented in Sects. 2.1 and 2.2. The multi-wavelength data set is presented in Sects. 2.3 and 2.4 for the X-ray and UV observations with *Swift* and in Sect. 2.5 for the optical observation with ATOM. The discussion in Sect. 3 focusses on the description of the SED in the framework of a synchrotron self-Compton (SSC) model.

Throughout this paper a ΛCDM cosmology with H_0 = 71 km s^{-1} Mpc^{-1}, Ω_Λ = 0.73 and Ω_M = 0.27 is assumed, resulting in a luminosity distance of D_L = 431 Mpc (Hogg 1999).

2. Observations and analyses

2.1. H.E.S.S. data set and analysis

H.E.S.S. is located in the Khomas Highland, Namibia (23°16′18″ S, 16°30′01″ E), at an altitude of 1800 m above sea level. H.E.S.S. is an array of imaging atmospheric Cherenkov telescopes. Each of four telescopes used in this study (H.E.S.S. phase 1) consists of a segmented 13 m diameter optical reflector (Bernlöhr et al. 2003) and a camera composed of 960 photomultipliers. The system works in a coincidence mode requiring the detection of an air shower by at least two telescopes (Funk et al. 2004).

SHBL J001355.9–185406 was observed with H.E.S.S. between MJD 54 653 and MJD 55 912 (July 6, 2008–December 17, 2011). Data were selected using the standard quality criteria (good weather, no hardware problem, see Aharonian et al. 2006), yielding an exposure of 41.5 h acceptance corrected live time at a mean zenith angle of 12.9°. The *Model* analysis (de Naurois & Rolland 2009) was performed with the *standard cuts* (threshold of 60 photo-electrons), leading to an energy threshold of E_{th} = 310 GeV for this observation. An excess of 153 γ-ray candidates has been found using the *Reflected-background* method (Aharonian et al. 2006) to subtract the background. The total numbers of ON- and OFF-source events are N_{ON} = 830 and N_{OFF} = 8190, respectively, with a background normalization factor $\alpha \simeq 0.083$. The source is detected with a significance of 5.5σ (Eq. (17) of Li & Ma 1983).

The distribution of excess events in a 2D map of 2° field of view centred on the source coordinates is given in Fig. 1. The fit of a point-like source, convolved with the H.E.S.S. point spread function (PSF), to the data results in the best-fit position of $\alpha_{J2000} = 00^h13^m52^s \pm 1.5^s_{stat} \pm 1.3^s_{sys}$ and $\delta_{J2000} = -18°53'29'' \pm 22''_{stat} \pm 20''_{sys}$, systematic uncertainties arising from telescope pointing. This is less than $2\sigma_{stat}$ away from the test position of SHBL J001355.9–185406 , derived from radio observations ($\alpha_{J2000} = 00^h13^m56^s \pm 0.05^s$ and $\delta_{J2000} = -18°54'06'' \pm 0.7''$, Condon et al. 1998). The source is compatible with a point-like source within the systematic uncertainties on the H.E.S.S. PSF. The distribution of ON-source events as a function of the square of the angular distance to the radio position is shown in Fig. 2 along with the OFF-source distribution.

[1] http://tevcat.uchicago.edu

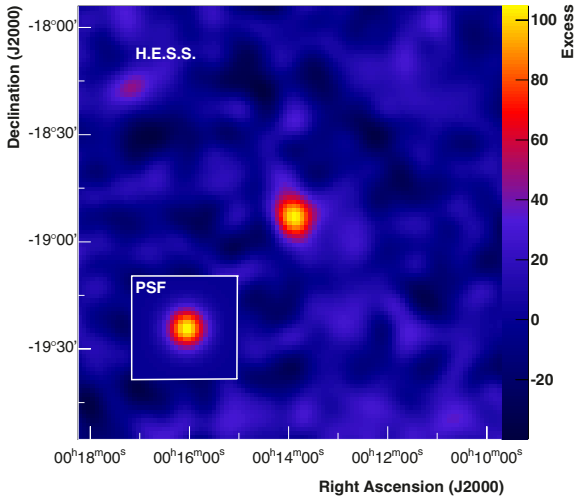

Fig. 1. Map of the γ-ray excess measured with the H.E.S.S. telescopes around the position of SHBL J001355.9–185406 in right ascension and declination (J2000). The map is smoothed with the H.E.S.S. PSF, shown in inset.

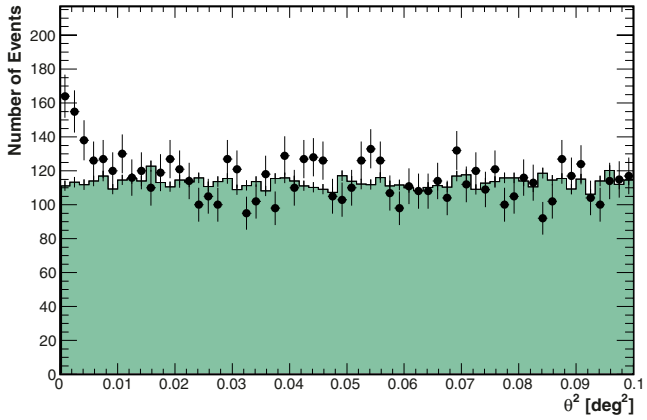

Fig. 2. Distribution of ON-source events (circles) as a function of the square of the angular distance θ^2 from the source position. A cut at $\theta = 0.1°$ is used to define the ON region with *standard cuts*. The distribution of normalized OFF-source (solid histogram) is flat and matches the distribution of the ON-source events at large θ^2, which reflects a proper background subtraction.

The VHE spectrum (Fig. 3), derived from the H.E.S.S. data using the forward-folding method in Piron et al. (2001), is compatible[2] with a simple power law of the form

$$\frac{\mathrm{d}N}{\mathrm{d}E} = (1.16 \pm 0.23_{\mathrm{stat}} \pm 0.23_{\mathrm{sys}}) \times 10^{-12} \left(\frac{E}{E_{\mathrm{dec}}}\right)^{-3.4 \pm 0.5_{\mathrm{stat}} \pm 0.2_{\mathrm{sys}}} \mathrm{cm}^{-2}\,\mathrm{s}^{-1}\,\mathrm{TeV}^{-1},$$

where the decorrelation energy is $E_{\mathrm{dec}} = 510\,\mathrm{GeV}$. The integrated flux above 310 GeV is $(8.3 \pm 1.7_{\mathrm{stat}} \pm 1.7_{\mathrm{sys}}) \times 10^{-13}$ photons cm^{-2} s^{-1}. The 1σ error contour was computed using Eq. (1) in Abdo et al. (2010b), and the systematic errors were evaluated following Aharonian et al. (2006). The analysis was cross-checked with an independent method (Becherini et al. 2011) giving compatible results.

A search for variability was performed on a period[3] time scale. The corresponding light-curve (Fig. 4, top panel) does not show any significant variations exceeding the experimental uncertainties, and the fit with a constant function yields a χ^2 probability of 7%. The fractional excess variance F_{var} (Vaughan et al. 2003) is compatible with zero at the 2σ level, and the 99% confidence level upper-limit is $F_{\mathrm{var}} < 2.57$.

[2] The χ^2/NDF is 25.1/19 for a corresponding probability of 15%.

[3] A period is defined as the time between two full moons (lunation).

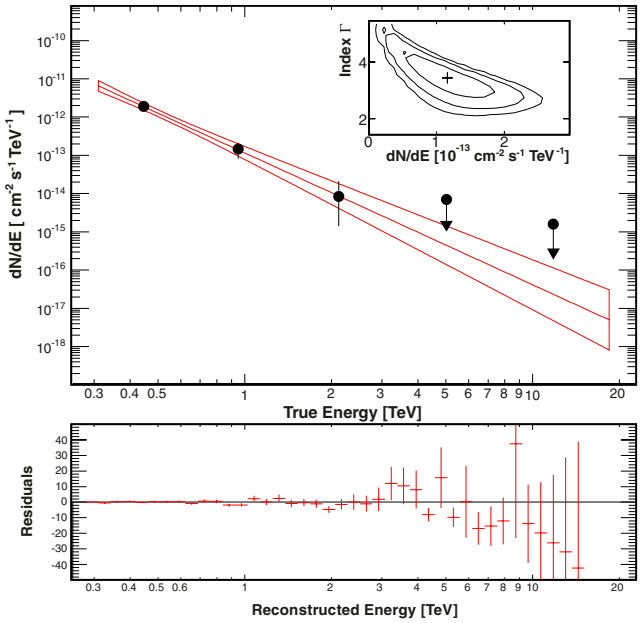

Fig. 3. Spectrum of SHBL J001355.9–185406 measured with H.E.S.S. using the *Model* analysis. *Top panel*: the butterfly represents the 1σ contour for the best-fit model. The spectrum is obtained with the forward-folding method in Piron et al. (2001). The data points are derived a posteriori and should be considered as residuals. For bins with a significance below 2σ, upper limits at the 95% confidence level are computed. The inset gives the 1, 2, and 3σ confidence levels in the power-law index vs differential flux at 1 TeV plane. *Bottom panel*: residuals of the fit, with the binning used in the forward-folding method.

2.2. Fermi-LAT data set and analysis

The LAT on-board the *Fermi* satellite is a pair conversion telescope sensitive to γ-rays between 20 MeV and 300 GeV. Its main characteristics and performance can be found in Atwood et al. (2009). The bulk of LAT observations are performed in an all-sky survey mode, where all objects are seen for about 30 min every 3 h.

Events passing the `SOURCE` selection (Ackermann et al. 2012) with a reconstructed energy between 300 MeV and 300 GeV have been considered in this analysis. The corresponding instrumental response functions (IRFs) `P7SOURCE_V6` and the latest public version of the ScienceTools (v9r27p1), available from the *Fermi* Science Support Center[4] web site, were used. A region of interest (ROI) of 15° radius around the radio coordinates of SHBL J001355.9–185406 was defined to perform a binned analysis (Mattox et al. 1996), implemented in the `gtlike` tool. Additionally, cuts were applied on the rocking angle of the spacecraft, which was required to be smaller than 52°, and on the zenith angle of the events, required to be smaller than 100°.

The model used to describe the observed emission consists of all the sources contained in the 2FGL catalogue within this ROI, an isotropic extragalactic diffuse component described with the file `iso_p7v6source.txt`, and the standard

[4] `http://fermi.gsfc.nasa.gov/ssc/data/analysis/`

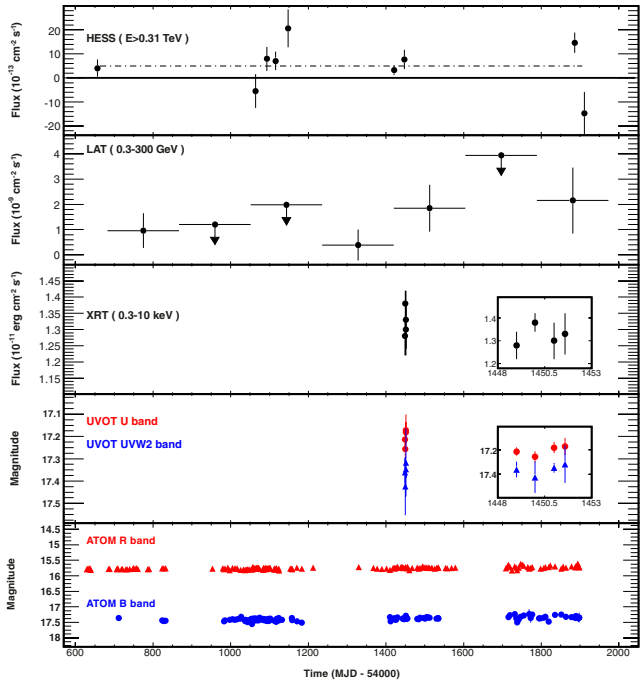

Fig. 4. Light-curves from observations at different wavelengths. From *top to bottom*: i) H.E.S.S. period-by-period integral-flux above 310 GeV. The dashed line is the mean flux level. The vertical bars give the statistical errors. ii) *Fermi*-LAT flux in the 300 MeV–300 GeV energy range. For time bins where the test-statistic is below 4, an upper limit at 95% confidence level is reported. iii) *Swift*-XRT flux in the 0.3−10 keV band. iv) *Swift*-UVOT measurement in *U* and *UVW2* bands. v) ATOM magnitudes in the *B* and *R* bands. The insets of panel iii and iv present a zoom in time around the *Swift* observations.

Galactic model `gal_2yearp7v6_v0.fits`. At the position of SHBL J001355.9–185406, a point-like source with a power-law model was added. The model of SHBL J001355.9–185406 has two free parameters: the differential flux at a fixed energy and the photon index Γ. The spectral parameters of sources within 3° of the SHBL J001355.9–185406 position, as well as the diffuse background normalizations and the variable and/or bright sources (namely 2FGL J2330.9–2144 and 2FGL J2345.0–1553), were left free to vary during the fitting procedure, whereas the other parameters were frozen to the 2FGL values.

Using 1290 days (≃3.5 years) of data, from August, 4 2008 to February, 12 2012 (MJD 54682 to MJD 55973), SHBL J001355.9–185406 is detected with a test statistic[5] (TS) of 34, which approximately corresponds to 5.5σ. This source was not detected by *Fermi*-LAT at the time of the 2FGL catalogue, which can be explained by its faint γ-ray flux. The coordinates derived with `gtfindsrc` are compatible with the radio position within 1σ. The source spectrum is described well by a power law with a differential flux of $(3.5 \pm 0.9_{\rm stat} \pm 0.7_{\rm sys}) \times 10^{-14}\,{\rm cm^{-2}\,s^{-1}\,MeV^{-1}}$ at the decorrelation energy $E_{\rm dec} = 2.90$ GeV. The photon index of the source is found to be $\Gamma = 1.96 \pm 0.20_{\rm stat} \pm 0.08_{\rm sys}$, yielding a total flux above 300 MeV of $(9.3 \pm 3.4_{\rm stat} \pm 0.8_{\rm sys}) \times 10^{-10}$ photons cm^{-2} s^{-1}. The photon with the highest detected energy that is very likely associated with the source[6] has an energy $E \approx 37$ GeV. Systematic uncertainties have been evaluated using the IRFs bracketing method (Abdo et al. 2009). A fit with a log-parabola function does not improve the overall results. The differential flux has also been measured in four energy bins (see Fig. 3) by performing a `gtlike` analysis for which the photon index of the source is frozen to the best-fit value. The last bin has a TS < 8 and a 95% confidence level upper limit has been computed.

Due to the faint emission of the source in the 300 MeV−300 GeV range, a light-curve with six-months-wide time-bins was computed using the `gtlike` analysis chain. This light curve is presented in the second panel of Fig. 4. Upper limits at the 95% confidence level were calculated for time bins with TS < 4. No significant variability can be measured on this time scale with $F_{\rm var} < 1.83$.

2.3. Swift-XRT data set and analysis

X-ray observations are usually an important part of characterizing the SED of blazars, since they probe the synchrotron radiation of the highest energy leptons. Target-of-opportunity observations with the space-based *Swift* (Burrows et al. 2005) X-ray observatory have been conducted in September 2010. Data taken in photon-counting (PC) mode are processed with the standard *xrtpipeline* tool from the `HEASOFT V6.12`, where a King function fit to the PSF shows no evidence of any pile-up in any of the four observations. Events and background extraction regions are defined with a 60-pixel radius circle (corresponding to ≈142″), with the latter centred near the former without overlapping. The *Swift*-XRT spectrum has been rebinned so as to have at least 20 counts per bin using `grppha`, yielding a usable energy range between 0.3 and 9.0 keV for the summed spectrum (0.3 and 5−7 keV for single observations). The weighted average column density of Galactic HI $N_{\rm H} = 2.13 \times 10^{20}\,{\rm cm^{-2}}$ has been extracted from the Leiden/Argentine/Bonn (LAB) Survey (Kalberla et al. 2005) using the nH tool from *HEASARC*[7]. Multiple model spectra are tested with `pyXspec 1.0`, using the response functions `swxpc0to12s6_20010101v013` and a dedicated ancillary response function (ARF) using `xrtmkarf` within `FTOOLS` at the location of the source in the field of view and with the summed exposure maps of the single observations. A single power law $F(E) = KE^{-\Gamma_X}$ poorly represents the fitted summed spectra, with $\chi^2_r = 1.23(179)$. An F-test probability (Bevington 1969) of 5×10^{-4} prefers the simplest smooth curved function, a three-parameter log-parabola $F(E) = KE^{-a-b\log(E)}$, for which all parameters are given in Table 1, including the spectrum obtained after summing all four event files in `xselect V2.4b` and building an exposure map with `ximage V4.5.1`. Similar conclusions were drawn by Massaro et al. (2011b) on this object with a different calibration. The source shows no indication of variability over the span of eight days (third panel of Fig. 4).

2.4. Swift-UVOT data set and analysis

The UVOT instrument (Roming et al. 2005) on-board *Swift* measured the UV emission of SHBL J001355.9–185406 in the bands U (345 nm) and UVW2 (188 nm) simultaneously with the X-ray telescope with an exposure of ∼1.5−2 ks each. The instrumental magnitudes and the corresponding fluxes (for conversion factors, see Poole et al. 2008) are calculated with `uvotmaghist` taking all photons into account from a circular region with a radius of 5″ (standard aperture for all filters). An appropriate

[5] See http://fermi.gsfc.nasa.gov/ssc/data/analysis/documentation/Cicerone/Cicerone_Likelihood/Likelihood_overview.html for a definition.

[6] A photon is considered as associated to the source if its reconstructed direction is within the 95% containment radius of the *Fermi*-LAT PSF.

[7] http://heasarc.gsfc.nasa.gov/cgi-bin/Tools/w3nh/w3nh.pl

Table 1. Parameters of power-law or log-parabolic fits to all four *Swift*-XRT observations, as well as the summed spectrum.

ObsID	Start time MJD-55000	Exposure [s]	Γ_X or a	b	K [10^{-3} cm^{-2} s^{-1} keV^{-1}]	χ^2_r(n.d.f.)	F-test	$F_{0.3-10\,\mathrm{keV}}$ [10^{-11} erg cm^{-2} s^{-1}]
00031806002	449.05	3783	1.95 ± 0.06	$0.30^{+0.14}_{-0.13}$	2.62 ± 0.09	1.15(55)	4×10^{-2}	1.28 ± 0.06
00031806003	449.98	4190	2.03 ± 0.04		2.46 ± 0.07	1.28(61)		1.38 ± 0.04
00031806004	451.05	3848	1.98 ± 0.05	$0.26^{+0.14}_{-0.13}$	2.46 ± 0.09	0.98(52)	5×10^{-2}	1.30 ± 0.08
00031806005	451.58	2745	2.02 ± 0.05		2.38 ± 0.08	0.80(39)		1.33 ± 0.09
sum		14 566	2.00 ± 0.03	0.23 ± 0.06	2.73 ± 0.05	1.15(178)	5×10^{-4}	1.36 ± 0.03

Notes. Column 4 gives either the power-law index Γ_X or the log-parabola value of a depending on which model best fits the data. Column 7 shows the reduced χ^2 value χ^2_r, Col. 8 the F-test probability for the log-parabolic model when it is preferred over the power law, and Col. 9 the estimation for the unabsorbed flux (using `cflux`) in the 0.3–10 keV range. The values of b and F-test are not provided when the log-parabola is not preferred.

Table 2. *Swift*-UVOT U and UVW2 measurements and time-averaged optical magnitudes and fluxes measured with ATOM in R, B, and I Bessel filters.

Filter	Energy [eV]	Magnitude	Flux [10^{-12} erg cm^{-2} s^{-1}]	$P(\chi^2_r)$ %
UVW2	6.6	17.4	1.99	63
U	3.6	17.2	1.44	94
B	2.88	17.5	3.26	99
R	1.77	15.8	6.09	19
I	1.37	14.2	8.36	

Notes. The last column gives the probability obtained when fitting the time series with a constant function. Magnitudes are not corrected for Galactic extinction, whereas fluxes are dereddened using the values of Schlegel et al. (1998).

background was determined from a circular region with radius 40″ near the source region without contamination of neighbouring sources. The measured UV fluxes are corrected for dust absorption using $E(B-V) = 0.0246$ mag[8] (Schlegel et al. 1998) and the $A_\lambda/E(B-V)$ ratios given in Seaton (1979).

The flux (Fig. 4, fourth panel), binned per observations, does not show any sign of variability in either of the two bands. Table 2 gives the chance probability obtained when fitting the data with a constant, as well as the average flux obtained when analysing all the observations together.

2.5. ATOM data set and analysis

The 75 cm Automatic Telescope for Optical Monitoring (ATOM, Hauser et al. 2004), located on the H.E.S.S. site has been used to monitor the optical emission of SHBL J001355.9–185406 in Bessell B, R, and I filter bands (Bessell 1990) over the last five years. The presented data have been obtained from MJD 54629 to MJD 55897 (June 6, 2008–December 2, 2011). A total of 138, 188, and 2 observations in B, R, and I bands, respectively, were carried out with an aperture of 4″ radius. The data were corrected for Galactic absorption using $A_\lambda(B) = 0.107$ mag, $A_\lambda(R) = 0.066$ mag and $A_\lambda(I) = 0.048$ mag (Schlegel et al. 1998) and the Bessell zero points (Bessell 1990) are used to convert the magnitude into flux units. The time-averaged flux in each band is given in Table 2 along with the corresponding energy.

Table 2 also gives the χ^2 probability obtained when fitting the time series with a constant function. The flux of the source (Fig. 4, fifth panel) is compatible with being constant over time in each band.

[8] http://irsa.ipac.caltech.edu/applications/DUST/

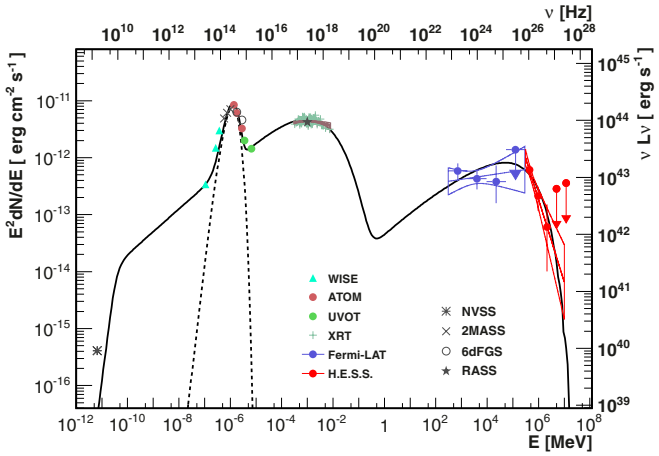

Fig. 5. Radio-to-TeV spectral energy distribution of SHBL J001355.9–185406 with ATOM (red circles, Table 2), *Swift*-UVOT (green circles), *Swift*-XRT (green cross + brown lines, Table 1), *Fermi*-LAT (blue), and H.E.S.S. (red) measurements. Archival data from NVSS, 2MASS, 6dFGS, and RASS are shown in grey. The dashed line is the black-body spectrum from the host galaxy at a temperature of 4500 K, and the black line shows the sum of the SSC calculation and the black-body spectrum.

3. Discussion

The broadband data presented in this work from ATOM, *Swift*, *Fermi*, and H.E.S.S., together with archival data from the NVSS (Condon et al. 1998), 2MASS (Skrutskie et al. 2006), 6dFGs (Jones et al. 2009), and RASS (Voges et al. 1996) catalogues are used to constrain physical characteristics of the source. Contemporaneous data from the Wide-field Infrared Survey Explorer (WISE, Wright et al. 2010) in the bands 3.4, 4.6, and 12 μm are also presented. The SED exhibits the usual two components, as can be noticed from Fig. 5.

The *Swift*-XRT data allow the synchrotron peak position to be located at $E_{\mathrm{s,\,peak}} = 1.00 \pm 0.07$ keV, a quite common feature of many objects in the SHBL catalogue, that peak in X-ray as mentioned by Giommi et al. (2005). Unfortunately, the source is too faint for the energy of the IC peak to be measured accurately, but Abdo et al. (2010a) found an empirical relation between the *Fermi* photon index and the peak position of the IC component. Applying the relation to SHBL J001355.9–185406 leads to $E_{\mathrm{ic,\,peak}} = 3.1^{+16.3}_{-2.7}$ GeV[9].

The spectral index found between the optical and UV waveband $\alpha_{\mathrm{o-uv}}$ is $\simeq -2.3$ which is not in agreement with the one

[9] The use of a relation derived on a population of sources might lead to large uncertainties but in the case of SHBL J001355.9–185406, a factor 10 in $E_{\mathrm{ic,\,peak}}$ would not affect the conclusions of this work.

observed between UV and X-ray, $\alpha_{\rm uv-x} \simeq 1.5$. The negative value of the former indicates that it does not originate from synchrotron emission of non-thermal particles but rather from the host galaxy thermal emission. This is supported by the non-variability of the ATOM light-curves and the good agreement of the optical flux with the archival data. Placing the source in a [3.4]−[4.6]−[12] μm colour−colour diagram (Massaro et al. 2011a) reveals that the infrared measurement is also dominated by this thermal emission. The host galaxy emission is modelled using a black-body, as in Katarzyński et al. (2003), with a temperature of 4500 K and a total luminosity of 1.43×10^{44} erg s^{-1}, which corresponds to 3.7×10^{10} times the luminosity of the Sun.

The non-thermal emission is modelled with a simple, time-independent, one-zone homogeneous SSC model (Band & Grindlay 1985). The emission zone is spherical with a radius R, moving relativistically towards the Earth with a Doppler factor δ. A population of leptons with a density $N_{\rm l}(\gamma)$ is responsible for the synchrotron emission by interacting with a uniform magnetic field B and for the γ-ray emission by IC scattering of the synchrotron photons.

Some properties of the SSC model can be assessed using the available data. A constraint on the maximal energy of the leptons can be found assuming the last bin in energy of *Swift*-XRT is a lower limit for the maximum energy reached by the synchrotron process $E_{\rm s,\,max}$. This gives (Rybicki & Lightman 1979)

$$E_{\rm s,\,max} \approx \frac{21\delta\hbar\gamma_{\rm max}^2 qB}{15(1+z)\sqrt{3}m_{\rm e}} \gtrsim 8\,{\rm keV}, \quad (1)$$

where q is the charge of the electron and B is in Gauss. Equation (1) implies $\gamma_{\rm max} \geq 9.7 \times 10^4\, B^{-1/2}\delta^{-1/2}$.

Since the same population of particles is responsible for the two spectral components and under the hypothesis that the IC scattering occurs in the Thomson regime, Eq. (4) of Tavecchio et al. (1998) reads as

$$B\delta = (1+z)\frac{8.6 \times 10^7 E_{\rm s,peak}^2}{E_{\rm ic,\,peak}} = 3.1 \times 10^4\ {\rm G}, \quad (2)$$

where the energies are expressed in eV. For a magnetic field B of 0.1 G, this leads to a Doppler factor of 3.1×10^5, which is unrealistic. For the photons of energy higher than $E_{\rm ic,\,peak}$, the scattering must occur in the Klein-Nishina regime in which case the leptons producing the highest energy detected follow $E_{\rm ic,\,max} = \frac{\delta}{1+z}\gamma_{\rm max} m_{\rm e}c^2 = 18$ TeV, which with the above constraint on $\gamma_{\rm max}$, in turn yields $B\delta^{-1} \geq 6.3 \times 10^{-8}$ G.

Even with the previous calculations, the SSC model is still not fully constrained by the data. To reduce the number of parameters, the density of leptons is described by a power law with an exponential cut-off of the form $N_{\rm e}(\gamma) \propto \gamma^{-p} \exp(-\gamma/\gamma_{\rm cut})$ which only has three parameters. An equipartition factor Q (defined as the ratio between the density of particle kinetic energy and the magnetic energy density (i.e. $Q = u_{\rm e}/u_B$)), that is as close to unity as possible has also been required, to minimize the total energy of the jet (see Ghisellini 2012). With this model, the minimum factor allowing a fit to the data is $Q = 50$, which rules out the equipartition and the jet is found to be particle-dominated. The same conclusions have been drawn for other sources, such as Mrk 421 (Abdo et al. 2011b) or Mrk 501 (Abdo et al. 2011a).

The SSC calculation, together with the thermal black-body component, is shown in Fig. 5, and parameters are given in Table 3. The attenuation by the extragalactic background light has been taken into account using the model of Franceschini et al. (2008). The index of the leptonic distribution is found to be $p = 2.2$ with a break at $\gamma_{\rm cut} = 5.0 \times 10^5$, for a total number of leptons of 2.0×10^{53}. The size of the emission region is $R = 3.5 \times 10^{16}$ cm, the Doppler factor $\delta = 10$, and the magnetic field $B = 0.05$ G (i.e. $U_B = 10^{-4}$ erg cm^{-3}), values that comply with the above-mentioned constraints. The minimum variability time scale achievable within this scenario is 1.4 days, which cannot be tested with H.E.S.S. or *Fermi* given the flux of the source.

Table 3. SSC parameters used to reproduce the SED of SHBL J001355.9–185406.

Parameters	Value
B [G]	0.05
R [cm]	3.5×10^{16}
δ	10
p	2.2
$\gamma_{\rm min}$	1
$\gamma_{\rm cut}$	5.0×10^5
$N_{\rm tot}$	2.0×10^{53}

Notes. The calculation is shown as a black line in Fig. 5.

To check that $\gamma_{\rm cut}$ can be related to the synchrotron cooling time or be acceleration effects, the comparison between the ratio of the light crossing time $\tau_{\rm c}$ in the emission zone rest-frame and the cooling time[10] $\tau_{\rm cool}$ can be used. Tavecchio et al. (1998) suggest that this ratio should be between 1 and 3. For the model presented here, this ratio is close to 1.8 and so is not possible to disentangle a radiative cooling break from a cut-off in the lepton distribution due to acceleration effects.

4. Conclusions

Dedicated observations using the H.E.S.S. telescopes have revealed a new HBL, SHBL J001355.9–185406, as a VHE γ-ray emitter, with a significance of 5.5σ. The source has a flux of about 0.6% of the Crab Nebula flux above 310 GeV, with a soft photon index $\Gamma = 3.4 \pm 0.5_{\rm stat} \pm 0.2_{\rm sys}$.

Using 3.5 years of *Fermi* data, the presence of a previously undetected counterpart in the HE range was found. Both HE and VHE spectra connect smoothly, leading to the conclusion that the same population of particles is likely to be responsible for the γ-ray emission from 300 MeV to a few TeV.

At lower energy, the optical measurements, which are contemporaneous with the H.E.S.S. and *Fermi*-LAT observations, are found to be constant over time and compatible with the data taken over the past decade. They are interpreted as thermal emission of the host galaxy and successfully reproduced by a black-body model.

An SSC model has been used to reproduce the non-thermal emission from radio to TeV energies. In this model, the γ-rays with energies above the γ-ray peak are produced by IC scattering showing evidence for Klein-Nishina suppression. Equipartition between the kinetic and the magnetic energy density is ruled out by the calculation, implying that the jet is dominated by the lepton kinetic energy.

The number of extragalactic sources jointly detected by the current generation of atmospheric Cherenkov telescopes and the *Fermi*-LAT is increasing rapidly, allowing the γ-ray sky from 100 MeV to a few TeV to be probed and the mechanisms responsible for the electromagnetic emission to be constrained. The knowledge of the non-thermal sky will increase with the

[10] The inverse of the cooling time for synchrotron dominated models is defined as $\tau_{\rm cool}^{-1} = \frac{4}{3}\frac{\sigma_{\rm T} c}{m_{\rm e}c^2}\gamma_{\rm cut}\, u_B$.

advent of H.E.S.S. 2 and the future Cherenkov Telescope Array (CTA). The ten-fold increased sensitivity of CTA with respect to current generation atmospheric Cherenkov telescopes and the possibility of performing an extragalactic survey (Dubus et al. 2013) will allow detection of hundreds of sources with fluxes of 1% of that the Crab Nebula. Such survey, together with ten years of *Fermi*-LAT data, will allow detailed population studies.

Acknowledgements. The support of the Namibian authorities and of the University of Namibia in facilitating the construction and operation of H.E.S.S. is gratefully acknowledged, as is the support by the German Ministry for Education and Research (BMBF), the Max Planck Society, the French Ministry for Research, the CNRS-IN2P3 and the Astroparticle Interdisciplinary Programme of the CNRS, the UK Particle Physics and Astronomy Research Council (PPARC), the IPNP of the Charles University, the South African Department of Science and Technology and National Research Foundation, and by the University of Namibia. We appreciate the excellent work of the technical support staff in Berlin, Durham, Hamburg, Heidelberg, Palaiseau, Paris, Saclay, and in Namibia in the construction and operation of the equipment. The *Fermi* LAT Collaboration acknowledges generous ongoing support from a number of agencies and institutes that have supported both the development and the operation of the LAT as well as scientific data analysis. These include the National Aeronautics and Space Administration and the Department of Energy in the US, the Commissariat à l'Énergie Atomique and the Centre National de la Recherche Scientifique/Institut National de Physique Nucléaire et de Physique des Particules in France, the Agenzia Spaziale Italiana and the Istituto Nazionale di Fisica Nucleare in Italy, the Ministry of Education, Culture, Sports, Science and Technology (MEXT), High Energy Accelerator Research Organization (KEK) and Japan Aerospace Exploration Agency (JAXA) in Japan, and the K. A. Wallenberg Foundation, the Swedish Research Council and the Swedish National Space Board in Sweden. Additional support for science analysis during the operations phase is gratefully acknowledged from the Istituto Nazionale di Astrofisica in Italy and the Centre National d'Études Spatiales in France. This research has made use of the NASA/IPAC Extragalactic Database (NED) which is operated by the Jet Propulsion Laboratory, California Institute of Technology, under contract with the National Aeronautics and Space Administration. This research has made use of the VizieR catalogue access tool, CDS, Strasbourg, France. This publication makes use of data products from the Wide-field Infrared Survey Explorer, which is a joint project of the University of California, Los Angeles, and the Jet Propulsion Laboratory/California Institute of Technology, funded by the National Aeronautics and Space Administration. The authors want to thank D. Paneque for the useful comments that improved the paper.

References

Abdo, A. A., et al. (*Fermi*-LAT Collaboration) 2009, ApJ, 707, 1310
Abdo, A. A., et al. (*Fermi*-LAT Collaboration) 2010a, ApJ, 716, 30
Abdo, A. A., et al. (*Fermi*-LAT Collaboration) 2010b, ApJ, 708, 1310
Abdo, A. A., et al. (*Fermi*-LAT Collaboration) 2011a, ApJ, 727, 129
Abdo, A. A., et al. (*Fermi*-LAT Collaboration) 2011b, ApJ, 736, 131
Ackermann, et al. (*Fermi*-LAT Collaboration) 2011, ApJ, 743, 171
Ackermann, et al. (Fermi-LAT Collaboration) 2012, ApJS, 203, 4
Aharonian, F. A. 2000, New Astron., 5, 377
Aharonian, F., Akhperjanian, A. G., Bazer-Bachi, A. R., et al. (H.E.S.S. Collaboration) 2006, A&A, 457, 899
Atwood, W. B., Abdo, A. A., Ackermann, M., et al. (*Fermi*-LAT Collaboration) 2009, ApJ, 697, 1071
Band, D. L., & Grindlay, J. E. 1985, ApJ, 298, 128
Becherini, Y., Djannati-Ataï, A., Marandon, V., Punch, M., & Pita, S. 2011, Astropart. Phys., 34, 858
Bernlöhr, K., Carrol, O., Cornils, R., et al. 2003, Astropart. Phys., 20, 111
Bessell, M. S. 1990, PASP, 102, 1181
Bevington, P. R. 1969, Data reduction and error analysis for the physical sciences
Burrows, D. N., Hill, J. E., Nousek, J. A., et al. 2005, Space Sci. Rev., 120, 165
Condon, J. J., Cotton, W. D., Greisen, E. W., et al. 1998, AJ, 115, 1693
Costamante, L., & Ghisellini, G. 2002, A&A, 384, 56
de Naurois, M., & Rolland, L. 2009, Astropart. Phys., 32, 231
Dermer, C. D., & Schlickeiser, R. 1993, ApJ, 416, 458
Dubus, G., Contreras, J. L., Funk, S., et al. 2013, Astropart. Phys., 43, 317
Franceschini, A., Rodighiero, G., & Vaccari, M. 2008, A&A, 487, 837
Funk, S., Hermann, G., Hinton, J., et al. 2004, Astropart. Phys., 22, 285
Ghisellini, G. 2011, in AIP Conf. Ser. 1381, eds. F. A. Aharonian, W. Hofmann, & F. M. Rieger, 180
Ghisellini, G. 2012 [arXiv:1202.5949]
Giommi, P., Piranomonte, S., Perri, M., & Padovani, P. 2005, A&A, 434, 385
Giommi, P., Padovani, P., Polenta, G., et al. 2012, MNRAS, 420, 2899
Hauser, M., Möllenhoff, C., Pühlhofer, G., et al. 2004, Astron. Nachr., 325, 659
Hofmann, W. 2010, The Astronomer's Telegram, 3007
Hogg, D. W. 1999 [arXiv:9905116]
Jones, D. H., Read, M. A., Saunders, W., et al. 2009, MNRAS, 399, 683
Kalberla, P. M. W., Burton, W. B., Hartmann, D., et al. 2005, A&A, 440, 775
Katarzyński, K., Sol, H., & Kus, A. 2003, A&A, 410, 101
Li, T.-P., & Ma, Y.-Q. 1983, ApJ, 272, 317
Mannheim, K. 1993, A&A, 269, 67
Massaro, F., Tramacere, A., Cavaliere, A., Perri, M., & Giommi, P. 2008, A&A, 478, 395
Massaro, F., D'Abrusco, R., Ajello, M., Grindlay, J. E., & Smith, H. A. 2011a, ApJ, 740, L48
Massaro, F., Paggi, A., Elvis, M., & Cavaliere, A. 2011b, ApJ, 739, 73
Mattox, J. R., Bertsch, D. L., & Chiang, J. 1996, ApJ, 461, 396
Nolan, P. L., Abdo, A. A., Ackermann, M., et al. 2012, ApJS, 199, 31
Padovani, P., & Giommi, P. 1995, ApJ, 444, 567
Piron, F., Djannati-Atai, A., Punch, M., et al. 2001, A&A, 374, 895
Poole, T. S., Breeveld, A. A., Page, M. J., et al. 2008, MNRAS, 383, 627
Punch, M., Akerlof, C. W., Cawley, M. F., et al. 1992, Nature, 358, 477
Roming, P. W. A., Kennedy, T. E., Mason, K. O., et al. 2005, Space Sci. Rev., 120, 95
Rybicki, G. B., & Lightman, A. P. 1979, Radiative processes in astrophysics
Schlegel, D. J., Finkbeiner, D. P., & Davis, M. 1998, ApJ, 500, 525
Schwope, A., Hasinger, G., Lehmann, I., et al. 2000, Astron. Nachr., 321, 1
Seaton, M. J. 1979, MNRAS, 187, 73
Skrutskie, M. F., Cutri, R. M., Stiening, R., et al. 2006, AJ, 131, 1163
Stickel, M., Padovani, P., Urry, C. M., Fried, J. W., & Kuehr, H. 1991, ApJ, 374, 431
Stocke, J. T., Morris, S. L., Gioia, I. M., et al. 1991, ApJS, 76, 813
Strong, A. W., Moskalenko, I. V., & Reimer, O. 2004, ApJ, 613, 962
Tavecchio, F., Maraschi, L., & Ghisellini, G. 1998, ApJ, 509, 608
Tavecchio, F., Ghisellini, G., Ghirlanda, G., Foschini, L., & Maraschi, L. 2010, MNRAS, 401, 1570
Urry, C. M., & Padovani, P. 1995, PASP, 107, 803
Vaughan, S., Edelson, R., Warwick, R. S., & Uttley, P. 2003, MNRAS, 345, 1271
Voges, W., Aschenbach, B., Boller, T., et al. 1996, IAU Circ., 6420, 2
Wright, E. L., Eisenhardt, P. R. M., Mainzer, A. K., et al. 2010, AJ, 140, 1868

[1] Universität Hamburg, Institut für Experimentalphysik, Luruper Chaussee 149, 22761 Hamburg, Germany
[2] Laboratoire Univers et Particules de Montpellier, Université Montpellier 2, CNRS/IN2P3, CC 72, Place Eugène Bataillon, 34095 Montpellier Cedex 5, France
[3] Max-Planck-Institut für Kernphysik, PO Box 103980, 69029 Heidelberg, Germany
[4] Dublin Institute for Advanced Studies, 31 Fitzwilliam Place, Dublin 2, Ireland
[5] National Academy of Sciences of the Republic of Armenia, Yerevan
[6] Yerevan Physics Institute, 2 Alikhanian Brothers St., 375036 Yerevan, Armenia
[7] Institut für Physik, Humboldt-Universität zu Berlin, Newtonstr. 15, 12489 Berlin, Germany
[8] Universität Erlangen-Nürnberg, Physikalisches Institut, Erwin-Rommel-Str. 1, 91058 Erlangen, Germany
[9] University of Durham, Department of Physics, South Road, Durham DH1 3LE, UK
[10] DESY, 15735 Zeuthen, Germany
[11] Institut für Physik und Astronomie, Universität Potsdam, Karl-Liebknecht-Strasse 24/25, 14476 Potsdam, Germany
[12] Nicolaus Copernicus Astronomical Center, ul. Bartycka 18, 00-716 Warsaw, Poland
[13] Landessternwarte, Universität Heidelberg, Königstuhl, 69117 Heidelberg, Germany
[14] APC, AstroParticule et Cosmologie, Université Paris Diderot, CNRS/IN2P3, CEA/Irfu, Observatoire de Paris, Sorbonne Paris Cité, 10 rue Alice Domon et Léonie Duquet, 75205 Paris Cedex 13, France
[15] Laboratoire Leprince-Ringuet, École Polytechnique, CNRS/IN2P3, 91128 Palaiseau, France
[16] Institut für Theoretische Physik, Lehrstuhl IV: Weltraum und Astrophysik, Ruhr-Universität Bochum, 44780 Bochum, Germany
[17] Institut für Astro- und Teilchenphysik, Leopold-Franzens-Universität Innsbruck, 6020 Innsbruck, Austria

[18] LUTH, Observatoire de Paris, CNRS, Université Paris Diderot, 5 place Jules Janssen, 92190 Meudon, France
[19] LPNHE, Université Pierre et Marie Curie Paris 6, Université Denis Diderot Paris 7, CNRS/IN2P3, 4 place Jussieu, 75252 Paris Cedex 5, France
[20] Institut für Astronomie und Astrophysik, Universität Tübingen, Sand 1, 72076 Tübingen, Germany
[21] DSM/Irfu, CEA Saclay, 91191 Gif-Sur-Yvette Cedex, France
[22] Astronomical Observatory, The University of Warsaw, Al. Ujazdowskie 4, 00-478 Warsaw, Poland
[23] Unit for Space Physics, North-West University, 2520 Potchefstroom, South Africa
[24] Harvard-Smithsonian Center for Astrophysics, 60 garden Street, Cambridge, MA 02138, USA
[25] School of Physics, University of the Witwatersrand, 1 Jan Smuts Avenue, Braamfontein, 2050 Johannesburg, South Africa
[26] Oskar Klein Centre, Department of Physics, Stockholm University, Albanova University Center, 10691 Stockholm, Sweden
[27] Université Bordeaux 1, CNRS/IN2P3, Centre d'Études Nucléaires de Bordeaux Gradignan, 33175 Gradignan, France
[28] Funded by contract ERC-StG-259391 from the European Community
[29] University of Namibia, Department of Physics, Private Bag 13301, Windhoek, Namibia
[30] School of Chemistry & Physics, University of Adelaide, 5005 Adelaide, Australia
[31] UJF-Grenoble 1/CNRS-INSU, Institut de Planétologie et d'Astrophysique de Grenoble (IPAG) UMR 5274, 38041 Grenoble, France
[32] Department of Physics and Astronomy, The University of Leicester, University Road, Leicester, LE1 7RH, UK
[33] Instytut Fizyki Jądrowej PAN, ul. Radzikowskiego 152, 31-342 Kraków, Poland
[34] Laboratoire d'Annecy-le-Vieux de Physique des Particules, Université de Savoie, CNRS/IN2P3, 74941 Annecy-le-Vieux, France
[35] Obserwatorium Astronomiczne, Uniwersytet Jagielloński, ul. Orla 171, 30-244 Kraków, Poland
[36] Toruń Centre for Astronomy, Nicolaus Copernicus University, ul. Gagarina 11, 87-100 Toruń, Poland
[37] Charles University, Faculty of Mathematics and Physics, Institute of Particle and Nuclear Physics, V Holešovičkách 2, 180 00 Prague 8, Czech Republic
[38] School of Physics & Astronomy, University of Leeds, Leeds LS2 9JT, UK